Investigation of solute–solvent interactions in a dithiophosphoro-organic carbohydrate derivative by means of X-ray analysis and solid state NMR

Marek J. Potrzebowski,*[a] Katarzyna Ganicz,[b] Włodzimierz Ciesielski,[a] Aleksandra Skowrońska,[b] Michał W. Wieczorek,[c] Jarosław Błaszczyk[c] and Wiesław Majzner[c]

[a] *NMR Laboratory, Polish Academy of Sciences, Centre of Molecular and Macromolecular Studies, 90-363 Łódź, Sienkiewicza 112, Poland*
[b] *Department of Heteroorganic Chemistry, Polish Academy of Sciences, Centre of Molecular and Macromolecular Studies, 90-363 Łódź, Sienkiewicza 112, Poland*
[c] *Technical University, Institute of General Food Chemistry, Stefanowskiego 4/10, 90-924 Łódź, Poland*

Received (in Cambridge, UK) 19th April 1999, Accepted 13th July 1999

Bis[6-*O*,6′-*O*-(1,2:3,4-diisopropylidene-α-D-galactopyranosyl)thiophosphoryl] disulfide **1** ($C_{48}H_{76}O_{24}P_2S_4$) crystallized from polar and/or nonpolar solvents forms different inclusion complexes and solvates. The X-ray data for complexes of **1** with propan-2-ol (**1a**) and acetone (**1b**) are reported. From DSC measurements it is apparent that with loss of the solvent, crystals undergo complex rearrangements below the melting point forming the **1c** modification. Each form is characterized by ^{31}P CP/MAS experiment. The analysis of the ^{31}P δ_{ii} principal elements of the chemical shift tensor suggests that distinction of δ_{33} for different modifications is related to O–H···S=P and C–H···S=P intermolecular contacts. ^{2}H NMR spectroscopy is employed to investigate the mechanism of phase reorientation and molecular dynamics of methyls of the isopropylidene blocking groups. At ambient temperature, the C_{3v} jump of the methyl group and additional small-amplitude motion of the five membered ring is deduced from line-shape analysis of a ^{2}H QUADECHO experiment. During the change of sample composition at 370 K, fast molecular motion of the methyl groups is observed while the S=P–S–S–P=S backbone remains rigid. From variable temperature ^{2}H T_1 inversion–recovery measurements it is concluded that the E_a of the C_{3v} jump strongly depends on molecular packing.

Introduction

The continuing development of the field of supramolecular chemistry is dependent on a thorough understanding of the mechanisms of different intermolecular contacts including hydrogen bonding, van der Waals, hydrophobic, electrostatic, aromatic–aromatic, dipole–dipole and solute–solvent interactions.[1,2] Recently, the weak hydrogen bonds, C–H···O, C–H···N, O–H···π, N–H···π, C–H···π, have attracted increasing attention due to their significance in crystal engineering, molecular recognition, self-organization of biomolecules and host–guest chemistry.[3,4] In our previous paper employing 1,6-anhydro-2-*O*-(tosyl)-4-*S*-(5,5-dimethyl-2-thioxo-1,3,2-dioxaphosphorinan-2-yl)-β-D-glucopyranose as a model compound and searching the Cambridge Structural Database (CSD) we revealed that C–H···S intermolecular contacts are not unusual for thiophosphoryl compounds.[5] We have found more examples of the C–H···S=P contact than for the analogous C–H···O=P interactions. This fact was explained in terms of hard and soft hydrogen bonds.[6,7] The S=P is a softer acceptor compared to the O=P unit which prefers to hydrogen bond with the soft donor C–H.

Procedures to analyze weak intermolecular interactions are strongly desired and in principle, a broad range of spectroscopic techniques can be applied. Among commonly used methods, recently solid state NMR spectroscopy has received considerable attention. Continuing our interest in understanding the mechanism of solute–solvent interactions for thiophosphoryl compounds, the formation of different crystallographic modifications, thermal stability, motional behavior of blocking groups and the influence of C–H···S hydrogen bonding on changes in phosphorus shielding parameters we report multi-nuclear, variable temperature solid state NMR, X-ray and DSC (differential scanning calorimetry) studies of bis[6-*O*,6′-*O*-(1,2:3,4-diisopropylidene-α-D-galactopyranosyl)-thiophosphoryl] disulfide **1** and its selectively deuterated derivative **1′** (Scheme 1). The method for the synthesis of **1** and

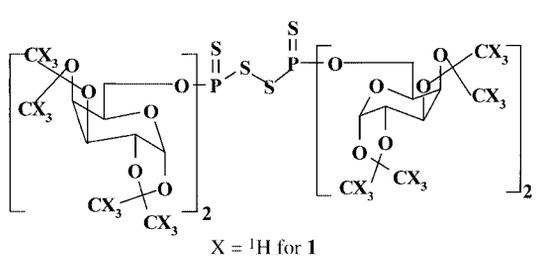

Scheme 1

preliminary structural studies in the solid phase were published elsewhere.[8]

Results

X-Ray diffraction studies

Crystallographic data and experimental details for disulfide **1** are shown in Table 1. Selected geometrical parameters for O–(S)P–S–S–P(S)–O units are presented in Table 2. The ORTEP

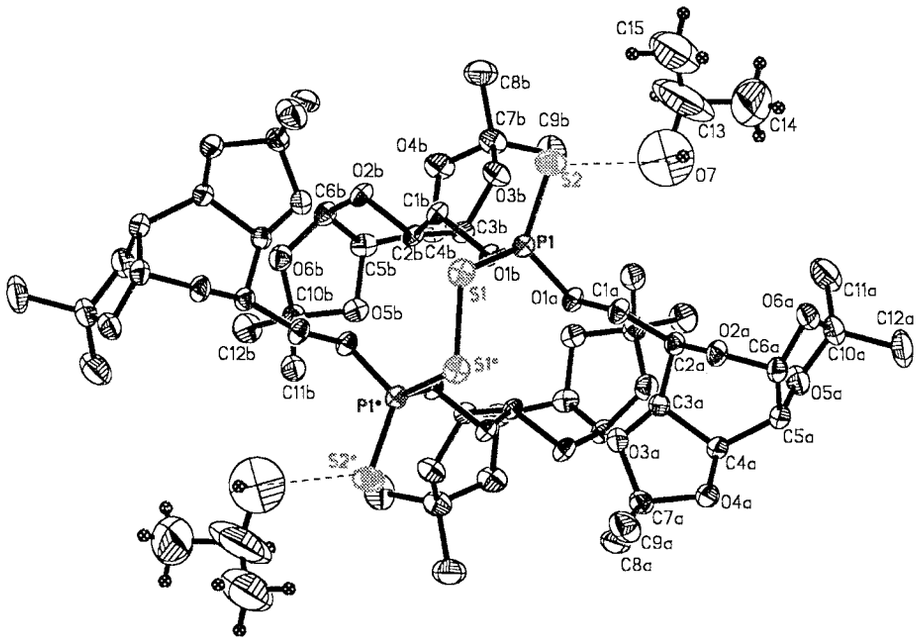

Fig. 1 Thermal ellipsoidal view and atom numbering scheme of **1a**. Molecular structure shows 20% probability displacement ellipsoids. Only one position of a hydroxy group in disordered solvent molecule is shown.

Table 1 Crystal data and experimental details for crystallographic modifications of bis[6-*O*,6′-*O*-(1,2 : 3,4-diisopropylidenegalactopyranosyl)-thiophosphoryl] disulfide

	1a	**1b**
Molecular formula	$C_{48}H_{76}O_{24}P_2S_4 \times 2(C_3H_8O)$	$C_{48}H_{76}O_{24}P_2S_4 \times 2(C_3H_6O)$
M_r	1347.5	1343.4
Crystallization solvent	Propan-2-ol	Acetone
Crystallographic system	Monoclinic	Trigonal
Space group	*C*2	$P3_2$
a/Å	29.412(1)	11.825(5)
b/Å	10.429(1)	11.825(7)
c/Å	11.945(1)	43.082(9)
α/°		90.00
β/°	105.871(5)	90.00
γ/°		120.00
V/Å^3	3524(5)	5216.9(39)
Z	2	3
D_c/g cm^{-3}	1.270	1.283
Measured reflections	4027	
Independent reflections	3746	
R_{int}	0.0139	0.1051
R_w	0.0476	0.3222
R	0.0412	0.1181

Table 2 Selected geometrical parameters (bond lengths, bond angles, torsional angles) of the S(O)P–S–S–S–P(O)S unit for **1a** and **1b** modification

	1a	**1b**
P=S	1.910(1) Å	1.908(3) Å
P–S	2.090(1) Å	2.076(3) Å
P–O	1.569(2) Å	1.576(5) Å
S–S	2.073(2) Å	2.071(3) Å
S=P–S	106.2(1)°	105.3(2)°
P–S–S	108.1(1)°	107.44(12)°
S=P–O	119.5(1)°	120.1(2)°
S–P–O	108.1(1)°	108.0(2)°
P–S–S–P	−79.3(1)°	−75.3(2)°
S–S–P=S	−158.7(1)°	−158.01(4)°
S–S–P–O	−29.3(1)°	−28.6(3)°

thermal ellipsoidal plots with the atom numbering scheme of disulfide **1a** (crystallized from propan-2-ol) are shown in Fig. 1.

1a crystallizes in the monoclinic system, space group *C*2. The asymmetric part of the unit cell contains a half-molecule of **1** and one molecule of propan-2-ol. The S=P–S–S–P=S backbone adopts *anti–anti* geometry with a S=P–S–S torsional angle equal to −158.7(1)°. The P–S and P=S bond lengths are found to be 2.090(1) Å and 1.910(1) Å, respectively and the S–S linkage is 2.073(2) Å. The S=P–S bond angle is 106.2(1)°. As seen, the geometric parameters reported in this work are very similar to values for other crystallographic modifications of **1** published elsewhere.[8]

The molecule of solvent is disordered, large thermal ellipsoids of carbon atoms and two positions of the hydroxy group (both positions with occupation factors of 50%) are assigned. The important interaction is hydrogen bonding between the O7–H7 hydroxy group and the S2 sulfur atom with the H7···S2 intermolecular distance equal to 3.18(5) Å, the O7···S2 length 3.33(3) Å and the O7–H7···S2 angle 135.7(5)°. It is also worth noting the interactions between C15–H15 of the methyl group from propan-2-ol and the S2=P unit (H15···S2 distance is 3.18(3) Å and C15–H15···S2

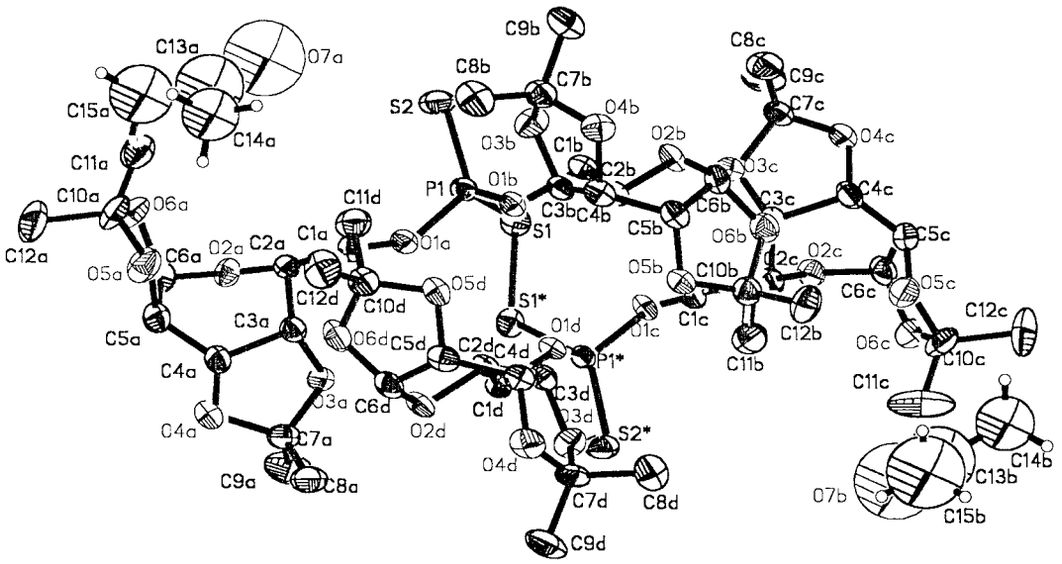

Fig. 2 Thermal ellipsoidal view and atom numbering scheme of the asymmetric part of the unit cell of **1b**. Molecular structure shows 20% probability displacement ellipsoids.

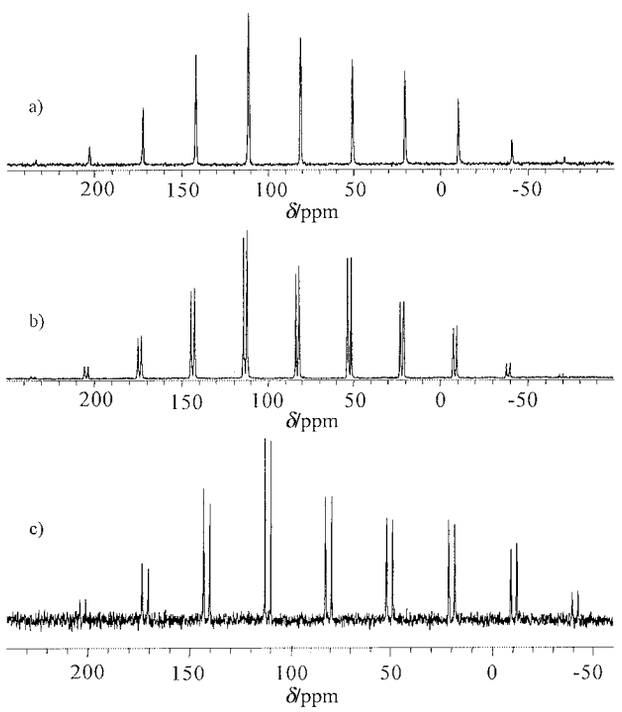

Fig. 3 121.49 MHz ^{31}H–^{31}P CP/MAS experimental spectra of (a) **1a** modification, (b) **1b** modification, (c) **1c** modification recorded at 370 K. The spectra have 4K data points with 10 Hz line broadening, a contact time of 1 ms, 100 scans and ν_{rot} = 3.7 kHz.

angle 174.6(4)°) and C8–H8 and C9–H9 from the methyl groups of the isopropylidene blocks of **1a** and the S2 unit (H82A · · · S2 and H92B · · · S2 distances are 3.16(2) Å, 3.12(2) Å and appropriate C8–H82A · · · S2 and C9–H92B · · · S2 angles are 160.5(4)°, 139.1(4)°).

1b crystallizes in the trigonal system, space group $P3_2$ (Fig. 2). The asymmetric part of the unit cell contains one molecule of **1** and two molecules of acetone. The geometry of the S=P–S–S–P=S skeleton defined by the appropriate torsional angles, bond angles and lengths is very similar to that established for **1a** (Table 2).

^{31}P CP/MAS solid state NMR studies

The room-temperature ^{31}P CP/MAS spectra of bis[6-*O*,6′-*O*-(1,2 : 3,4-diisopropylidene-α-D-galactopyranosyl)thiophosphoryl] disulfide crystallized from propan-2-ol (**1a**) and acetone (**1b**) are displayed in Fig. 3a and Fig. 3b, respectively. Both spectra show a set of spinning sidebands from the large chemical shielding anisotropy (CSA). The phosphorus can be considered as an isolated nucleus, because adjacent atoms in a tetrahedral arrangement are zero spin nuclei. The interactions with active isotopes of sulfur, carbon and oxygen at natural abundance are below detectable limits. The dipolar coupling from protons of galactopyranoses was eliminated by proton decoupling during data acquisition. The principal components of the ^{31}P chemical shift tensors δ_{ii} were calculated from spinning sideband intensities employing the WINMAS program that is based on the Herzfeld–Berger algorithm.[9,10] The calculated values of principal tensors elements δ_{ii} and shielding parameters are given in Table 3.

At higher temperatures **1a** and **1b** are not stable and a change of sample composition below the melting point is observed. Variable temperature (VT) ^{31}P CP/MAS revealed that in both cases, owing to thermal processes, the spectra at 373 K became very similar and a new modification, **1c**, is formed. The isotropic part of the spectrum of **1c** (Fig. 3c) is represented by two resonances separated by 3.0 ppm (86.3 ppm and 83.3 ppm). As concluded from ^{13}C CP/MAS spectra these changes are due to migration of solvent molecules from the crystal lattice (Fig. 4). With a gradual increase in temperature, in the range 300–370 K, the intensity of the diagnostic signals of the solvents (methyl groups of propan-2-ol, $\delta_{^{13}C}$ = 26 ppm, for **1a** and methyl $\delta_{^{13}C}$ = 30.5 ppm and carbonyl group of acetone, $\delta_{^{13}C}$ = 204 ppm, for **1b**) decreases.

Fig. 5 shows how complicated the pathway from **1b** (Fig. 5a) to **1c** (Fig. 5d) is. Figs. 5b and 5c display the ^{31}P CP/MAS spectra recorded at room temperature (only the isotropic part) for sample **1b** kept 24 and 48 hours at 320 K under vacuum. From these studies it is apparent that migration of solvent causes significant changes in the crystal lattice of the host and the thermal phase reorientation of **1** has only a few stages.

DSC studies

DSC profiles (Fig. 6) show that **1a** and **1b** release the guest molecules over a wide temperature range with a peak temperature of 377 K and 357 K, respectively. These temperatures are remarkably high in comparison to the boiling point of pure guest liquid (355 K for propan-2-ol and 329 K for acetone), indicating that the guest molecules are strongly held within the crystal lattice.

It is interesting to note that DSC profiles show not only

Table 3 ^{31}P chemical shift parameters for bis[6-*O*,6′-*O*-(1,2:3,4-diisopropylidene-α-D-galactopyranosyl)thiophosphoryl] disulfide **1**

Compound crystallized (solvent)	δ_{iso} (ppm)	δ_{11} (ppm)	δ_{22} (ppm)	δ_{33} (ppm)	$\lvert\Delta\delta\rvert$ (ppm)	Ω (ppm)	η	κ
1 propan-2-ol (298 K)	83.4	194.3	99.3	−43.2	190	238	0.75	0.20
1 propan-2-ol (373 K)	86.3	196.9	104.7	−42.6	193	240	0.72	0.23
	83.3	195.5	97.6	−43.2	190	239	0.77	0.18
1 acetone (298 K)	86.2	197.6	97.1	−36.0	183	234	0.82	0.14
	84.2	191.2	91.5	−30.2	172	221	0.87	0.10
1 acetone (343 K)	86.1	195.4	101.7	−38.7	187	234	0.75	0.20
	84.5	192.4	96.7	−35.6	180	228	0.80	0.16
	81.0	193.0	103.0	−47.1	195	240	0.69	0.25
1 acetone (373 K)	86.4	196.7	107.3	−44.9	197	242	0.68	0.26
	83.4	193.0	104.2	−47.1	196	240	0.68	0.26

Estimated errors in δ_{11}, δ_{22} and δ_{33} are ±2 ppm; errors in δ_{iso} are ±0.2 ppm. The principal components of the chemical shift tensor are defined as follows; $\delta_{11} > \delta_{22} > \delta_{33}$. The isotropic chemical shift is given by $\delta_{iso} = (\delta_{11} + \delta_{22} + \delta_{33})/3$.

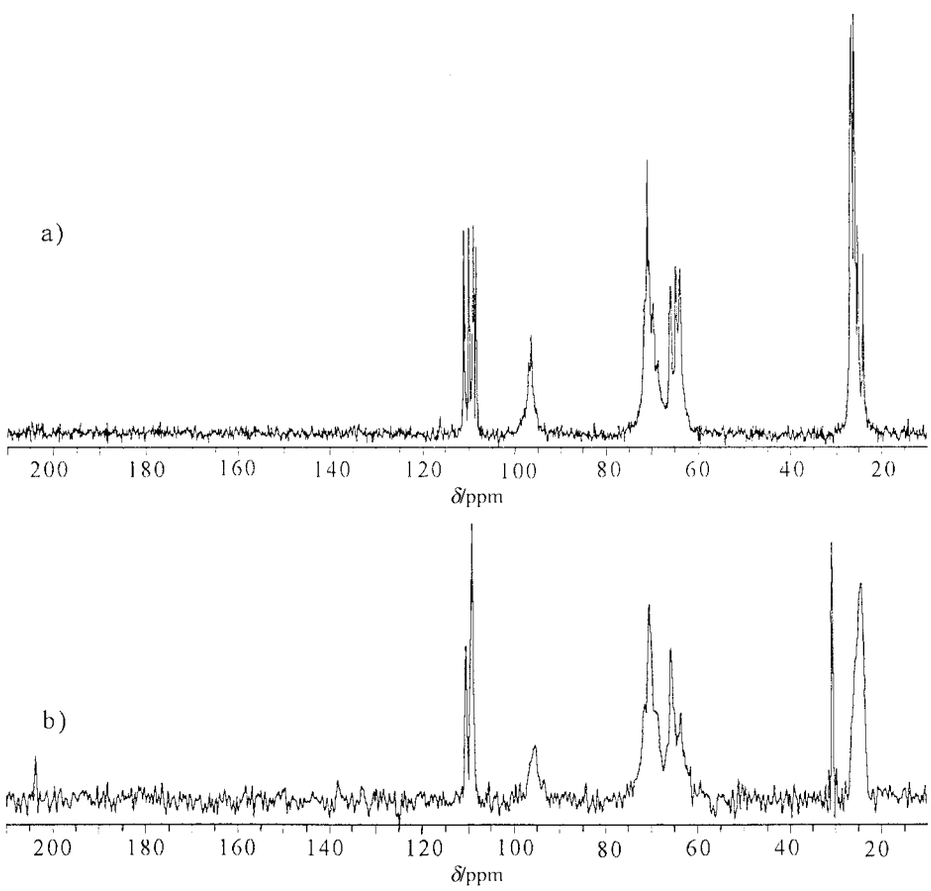

Fig. 4 75.46 MHz ^{1}H–^{13}C CP/MAS experimental spectra of (a) **1a** modification, (b) **1b** modification. The spectra have 4K data points with 10 Hz line broadening, a contact time of 1 ms, 1K scans and ν_{rot} = 3.7 kHz.

endothermic peaks which demonstrate guest releasing but also apparent exothermic peaks which correspond to phase alternation. In particular, it can be seen for sample **1b** where these effects are clear cut. The case of sample **1a** is more complex because two processes, endothermic releases of propan-2-ol and phase reorientation, overlap. After releasing the guest species, the **1a** and **1b** crystals behave very similarly, starting to melt at 425 K, giving the endothermic peak at 427 K.

In order to understand in detail the mechanism of thermal processes for **1**, further results were obtained from ^{2}H line shape analysis and inspection of dynamic parameters for deuterium labeled models.

^{2}H solid state NMR studies

The spectrum of selectively deuterium labeled methyl groups of bis{6-*O*,6′-*O*-[1,2:3,4-di(isopropylidene-d_6)-α-D-galactopyranosyl]thiophosphoryl} disulfide crystallized from propan-2-ol (**1′a**) is shown in Fig. 7.

The simulation procedure yielded the motionally averaged value of the asymmetry parameter $\eta_{eff} = 0.01$ and the quadrupole coupling constant QCC effective value $(e^2qQ/h)_{eff}$ is found to be 51 kHz. The value of the effective coupling constant indicates that the methyl groups have a correlation time in the fast limit ($\tau_c \leq 10^{-8}$ s).[11] Moreover, on varying the interval between $\pi/2$ pulses in the quadrupole echo pulse sequence from 20 to 120 μs, little intensity loss and no distortion of the powder line shape were observed. This experiment excluded the intermediate exchange of anisotropic T_2s in the range $10^{-4} \leq \tau_c \leq 10^{-6}$ s. The small quadrupole coupling constant is a result of fast rotational motion around a pseudo-threefold spinning axis. For tetrahedral geometry the static QCC value is reduced by a factor of 1/3. Studies of model compounds show that deuterons for static aliphatic groups have coupling constants of

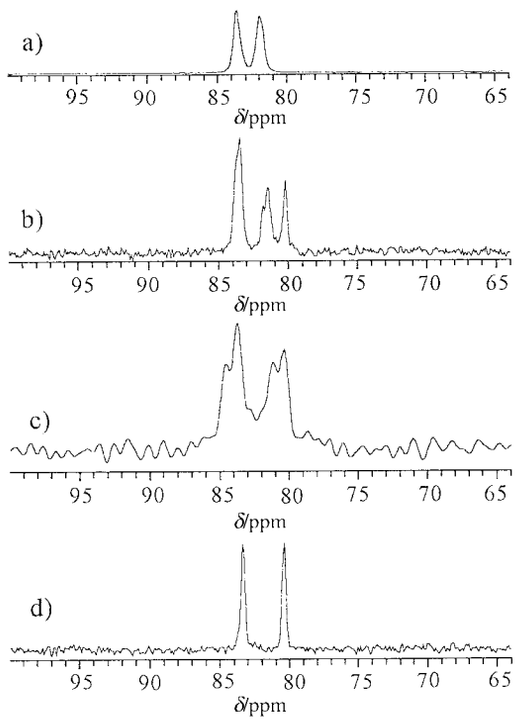

Fig. 5 Isotropic part of the 121.49 MHz ^{1}H–^{31}P CP/MAS spectra of **1b** modification kept under vacuum at 320 K for (a) 1 hour, (b) 24 hours, (c) 48 hours, (d) 5 days. The spectra have 4K data points with 10 Hz line broadening, a contact time of 1 ms, 100 scans and $\nu_{rot} = 3.7$ kHz.

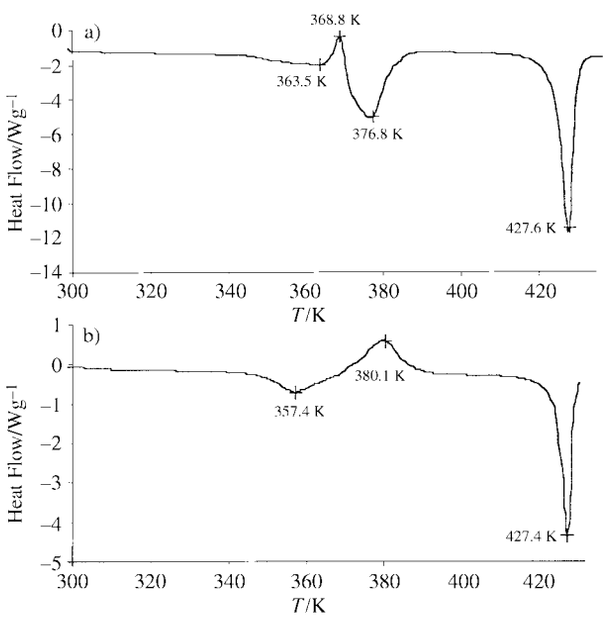

Fig. 6 DSC profile of (a) **1a** modification, (b) **1b** modification.

ca. 168 kHz and an asymmetry parameter $\eta = 0$ with the unique tensor axis lying parallel to the internuclear vector.[12] The value found here, 154 kHz, obtained by multiplying the effective (motionally averaged) quadrupole coupling constants (51 ± 1 kHz) by a factor of 3 is smaller than $(e^2qQ/h)_{static}$. This value may reflect an additional small-amplitude motion of the five membered ring.

Fig. 8 displays the inversion recovery ^{2}H NMR spectra of **1′a** at 223 K. As reported by Torchia and Szabo investigation of the spin-lattice relaxation time (T_1) may allow rotational diffusion or threefold jumps about the C_3 axis to be distinguished.[13] When the C–^{2}H bond jumps between three equivalent sites, $\tau_c = (3k)^{-1}$, the line shape is axially symmetric, while T_1 depends

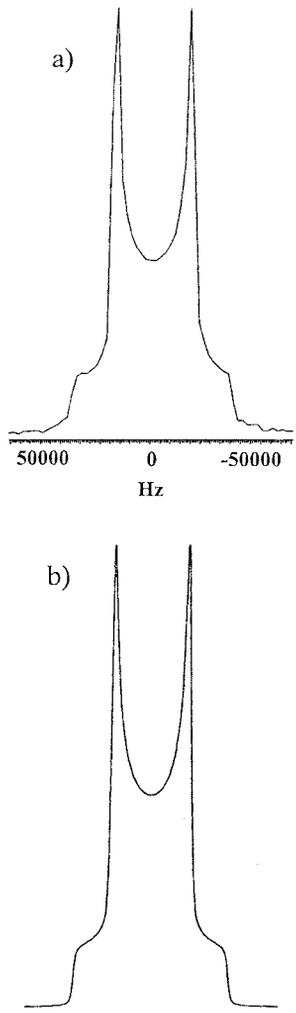

Fig. 7 (a) 46.07 MHz ^{2}H QUADECHO NMR spectrum of bis{6-*O*,6′-*O*-[1,2:3,4-di(isopropylidene-d_6)-α-D-galactopyranosyl]thiophosphoryl} disulfide crystallized from propan-2-ol (**1′a** modification) recorded at room temperature. The spectrum has 2K data points with 200 Hz line broadening, and 100 scans. (b) Calculated spectrum with $QCC_{eff} = 51$ kHz and $\eta_{eff} = 0.01$. The line shape was calculated using the MXQET program on a Silicon Graphics computer.[20]

on both polar angles which define the orientation of the applied static field in the crystal axis system. In a powder pattern a unique T_1 cannot be assigned to each frequency which means that different parts of the powder pattern relax differently for a three-site jump model.

The ^{2}H spin-lattice relaxation times, T_1, measured at several temperatures ranging from 195 K to 300 K, and other spectral parameters are collected in Table 4. The correlation times, assuming the threefold model, were calculated according to equations given elsewhere.[13]

Discussion

Our results clearly demonstrate that dynamic solute–solvent processes in the crystal lattice of **1** greatly complicate the X-ray data analysis. We were not able to refine the structure of **1b** with sufficient accuracy. In the crystal structure of **1b**, the host disulfide molecules form a well defined crystal structure base while the acetone molecules are located very loosely. This is the main factor making impossible the refinement of the structure of **1b** to low values of the *R*-factor. Three room temperature data sets and one low temperature set (123 K) have been collected. For the best data set the structure could be refined to the *R*-factor of 0.118. During low temperature data collection using a CCD detector, observation of a very weak satellite in

Table 4 Averaged ^{2}H spin-lattice relaxation times, correlation times, quadrupole splitting and activation energies for bis[6-*O*,6′-*O*-(1,2:3,4-diisopropylidene-α-D-galactopyranosyl)thiophosphoryl] disulfide **1**

	Crystallographic modification **1′a**			Crystallographic modification **1′b**			Crystallographic modification **1′c**		
Temperature/K	T_1/s	$\tau_c/10^{-12}$ s	Frequency separation between the two singularities/kHz	T_1/s	$\tau_c/10^{-12}$ s	Frequency separation between the two singularities/kHz	T_1/s	$\tau_c/10^{-12}$ s	Frequency separation between the two singularities/kHz
193	7.80	24.9	40.5	5.93	32.7	43.2	2.56	75.8	40.0
223	12.54	15.5	42.5	11.79	16.4	40.5	6.04	32.1	40.5
243	13.42	41.4	40.5	17.19	11.3	40.5	8.74	22.2	40.0
273	26.36	7.36	37.8	39.51	4.91	39.8	21.87	8.87	37.5
293	42.82	4.53	37.5	48.98	3.96	39.3	47.13	4.12	37.5
E_a/kJ mol^{-1}		9.50			10.15			13.2	

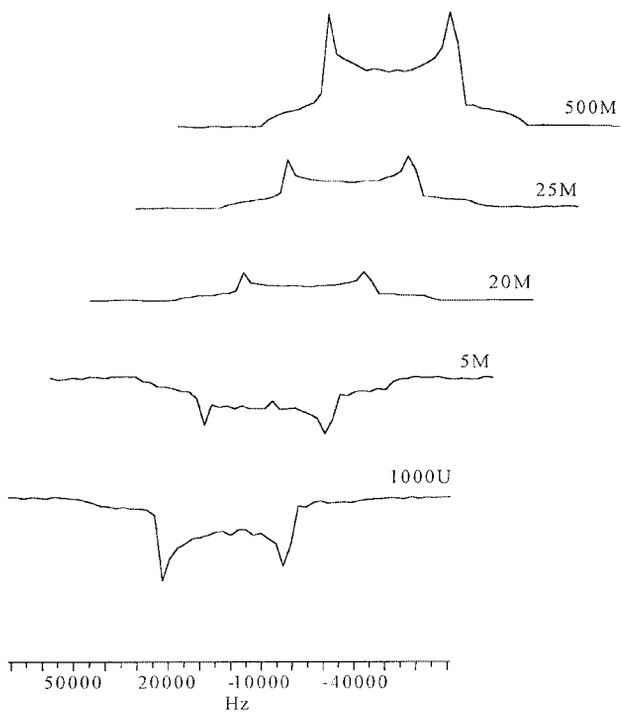

Fig. 8 46.07 MHz inversion–recovery ^{2}H NMR spectra of **1′a** modification recorded at 223 K using π–*T*–π/2–τ_1–π/2–τ_2–*acquire* pulse sequence.

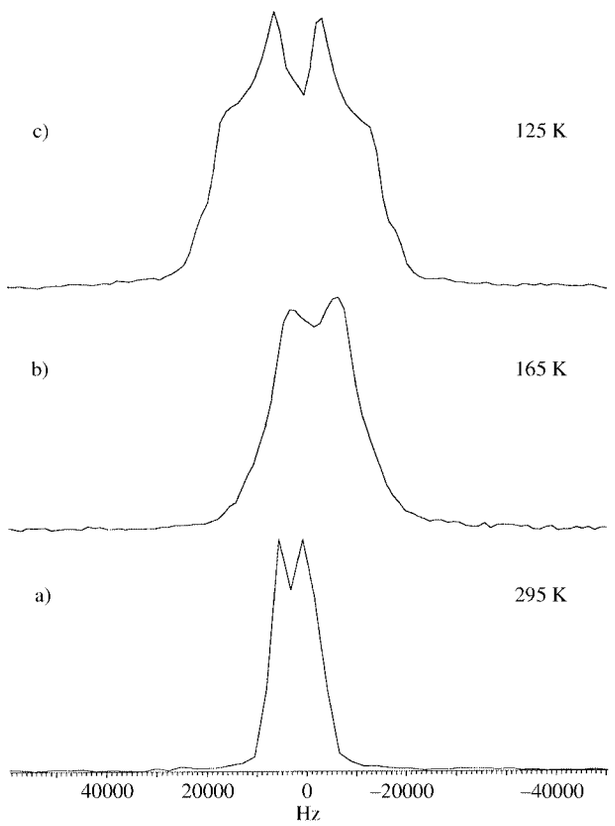

Fig. 9 46.07 MHz ^{2}H QUADECHO NMR spectrum of acetone-d_6 occluded in crystal lattice of **1b** modification recorded at (a) 300 K, (b) 165 K and (c) 125 K. The spectra have 2K data points with 200 Hz line broadening, and 100 scans.

the *c* direction suggests the formation of the substructure. From our measurements we conclude that despite the high level of the *R*-factor the geometrical parameters of the disulfide moiety are acceptable. The observation regarding the dynamics of the guest molecule is consistent with ^{2}H NMR studies of acetone-d_6 occluded in a crystal lattice.

Fig. 9 displays the ^{2}H QUADECHO spectra recorded in the temperature range from 295 K to 125 K. At 295 K (Fig. 9a) the splitting between the singularities of the quadrupole doublet is only 5 kHz. With the decrease in temperature the molecular motion of the guest molecule is slowed down, but even at 125 K acetone shows great mobility. Splitting between the singularities is found to be 10 kHz (Fig. 9c).

^{2}H NMR studies of deuterium labeled **1′** disulfide unambiguously revealed that not only solvents occluded in the crystal lattice are under fast regime exchange but the sugar residue also undergoes the dynamic processes. From ^{13}C T_1 data published by Dais *et al.* it is known that five membered isopropylidene blocking groups of sugars undergo complex molecular motion in the liquid phase.[14,15] The hindered rotation of methyl groups with librational reorientation of the isopropylidene ring and a puckering motion of the sugar ring was proved. In case of sample **1**, from ^{2}H line shape analysis of the quadrupolar doublet in the solid state, a C_{3v} jump of the methyl group and a small amplitude motion of the five membered ring are apparent.

As shown in the previous section the thermal process modifies **1a** and **1b** complexes in a similar way and as a result the **1c** modification is obtained. Analysis of the ^{2}H NMR spectrum for **1′c**, recorded at 370 K (Fig. 10a) shows apparent differences. The ^{2}H NMR line shape of **1′c** at 370 K is a superposition of a Pake doublet (crystalline phase) and a motionally narrowed spectrum which corresponds to methyl-d_3 groups under a very fast exchange regime. It is clear from the data that the process of thermal phase transition is related to the large amplitude motion of the isopropylidene groups. The open question is the dynamics of the sugar rings at higher temperature. From our experiment the reorientation of galactopyranose can not be excluded.

The apparent activation energies E_a calculated from the Arrhenius plot, assuming that the C_{3v} jump of the methyl

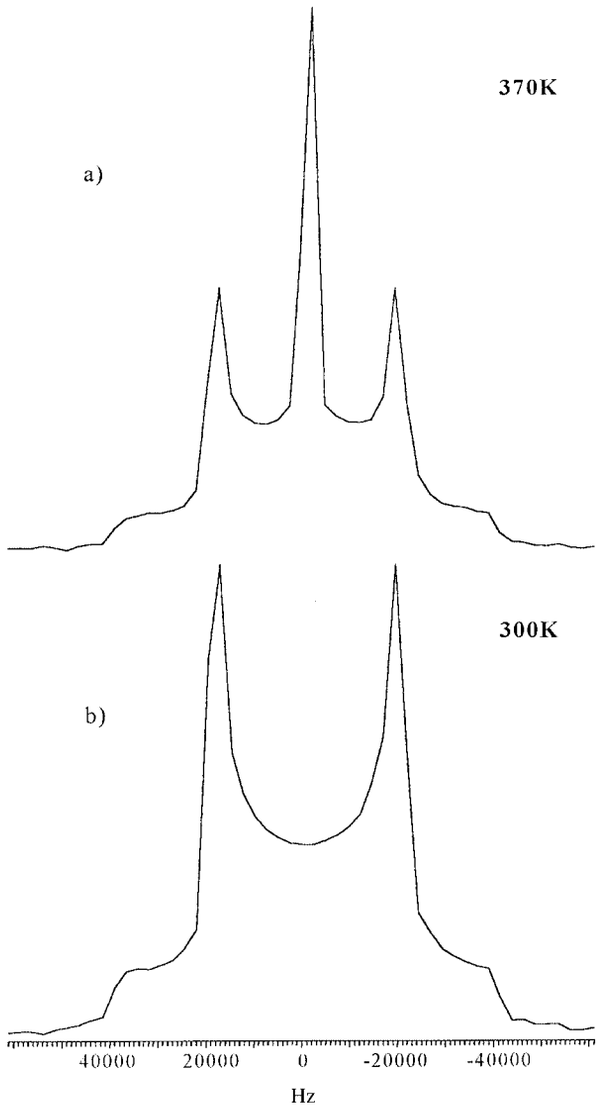

Fig. 10 46.07 MHz ^{2}H QUADECHO NMR spectrum of (a) **1′c** modification recorded at 370 K, (b) **1′c** modification recorded at room temperature. The spectra have 2K data points with 200 Hz line broadening, and 100 scans.

groups is the only activated process, were found to be 9.50 kJ mol^{-1} for **1′a**, 10.15 kJ mol^{-1} for **1′b** and 13.2 kJ mol^{-1} for **1′c**. These values are comparable to those reported for other biological systems.[12,16,17] It is obvious from this work that molecular packing has a significant influence on the distinction of E_a parameters for the different crystallographic modifications of **1**.

In contrast to solvents occluded in a crystal lattice as well as isopropylidene blocking groups, the S=P–S–S–P=S backbone remains rigid over a broad temperature range as concluded from a variable temperature ^{31}P NMR experiment. Each crystallographic modification can be easily recognized by ^{31}P CP/MAS experiment. Inspection of the results collected in Table 3 shows differences between **1a** and **1b**. At room temperature **1a** is represented by a single resonance in an isotropic part (δ_{iso} = 83.4 ppm) while **1b** shows two lines separated by 2 ppm (δ_{iso} equal to 86.2 and 84.2 ppm). Such results are consistent with the X-ray data. For **1a**, in the *C*2 space group with twofold symmetry about the S–S bond, one crystallographically nonequivalent phosphorus site P1 is established. For **1b**, in the noncentrosymmetric $P3_2$ space group, two crystallographically nonequivalent phosphorus sites (P1 and P2) are seen as a whole molecule in an asymmetric unit.

The differences are monitored for δ_{ii} parameters. The most significant distinction is seen for δ_{22} and δ_{33} components during the sample heating. These changes are due to a molecular packing effect as well as P=S···H–C and/or P=S···H–O intermolecular contacts. Similar differences in δ_{33} parameters were observed for other dithiophosphoroorganic sugar derivatives. The mechanism and nature of such distinctions are discussed elsewhere.[5]

Experimental

Synthesis of bis{6-*O*,6′-*O*-[1,2:3,4-di(isopropylidene-d_6)-α-D-galactopyranosyl]thiophosphoryl} disulfide 1′

The slurry of anhydrous α-D-galactose (782 mg, 4.34 mmol), powdered anhydrous cupric sulfate (1.73 g, 10.86 mmol), and conc. sulfuric acid (9.2×10^{-2} ml, 1.72 mmol) in 60 ml of dry acetone-d_6 was stirred for 24 hours at rt, filtered and washed with anhydrous acetone-d_6. The filtrate was neutralized by shaking with powdered calcium hydroxide to achieve pH 7.0. The mixture was filtered and the filtrate was evaporated under reduced pressure. The expected product was obtained by distillation under vacuum (130 °C/0.05 mmHg). Yield 58%.

710 mg (2.61 mmol) of 1,2:3,4-di(isopropylidene-d_6)-α-D-galactopyranose and 290 mg (0.65 mmol) of phosphorus pentasulfide were suspended in 100 ml of dry toluene. 180 µl (1.30 mmol) of triethylamine was added dropwise at rt. The mixture was refluxed for 5 h, evaporated under reduced pressure and extracted with toluene. The triethylamine salt of 6-*O*,6′-*O*-[1,2: 3,4-di(isopropylidene-d_6)-α-D-galactopyranosyl]dithiophosphoric acid was oxidized with iodine in a mixture of toluene–water. The toluene solution of product was dried over magnesium sulfate. The solvent was removed under vacuum. The crude product was recrystallized from a mixture of benzene–hexane at −15 °C. Yield 60%. ^{1}H NMR ($CDCl_3$), δ 4.07–4.17 (m, 1H), 4.23–4.41 (m, 4H), 4.57–4.65 (m, 1H), 5.51 (dd, J = 4.95 Hz, J = 1.59 Hz, 1H).

NMR measurements

Cross-polarization magic angle spinning solid state ^{31}P and ^{2}H NMR spectra were recorded on a Bruker 300 MSL instrument with high-power proton decoupling at 121.496 MHz for ^{31}P and 46.07 MHz for ^{2}H. Powder samples of **1** were placed in a cylindrical rotor and spun at 2.0–4.5 kHz. For the ^{31}P experiments, the field strength for ^{1}H decoupling was 1.05 mT, a contact time of 5 ms, a repetition of 6 s and spectral width of 50 kHz were used and 8K data points represented the FID. Spectra were accumulated 100 times which gave a reasonable signal-to-noise ratio. ^{31}P chemical shifts were calibrated indirectly through bis(dineopentoxythiophosphoryl) disulfide set at 84.0 ppm.

The principal elements of the ^{31}P chemical shift tensor and shielding parameters were calculated employing the WIN-MAS program. The details describing the method and accuracy of calculations are exhaustively discussed elsewhere.[9,10] The principal components δ_{ii} were used for calculation of the chemical shift parameters, anisotropy $\Delta\delta$, asymmetry η, span Ω and skew κ.[18]

Solid-state ^{2}H NMR experiments were carried out using the eight-step phase-cycled quadrupole echo pulse sequence. The 90° pulse times were typically less than 5 µs, and the delays between pulses in the sequence were 30 and 33 µs, respectively. Data acquisition was initiated prior to the top of the quadrupolar echo. Time domain data were shifted to the echo maximum prior to Fourier transformation.[19] Lorentzian line broadening of 50–256 Hz was used to obtain an adequate signal-to-noise ratio. The simulation of the ^{2}H line shape was carried out using the MXQET program on a Silicon Graphics computer.[20]

The inversion–recovery pulse sequence was employed for the determination of the deuterium spin-lattice relaxation times

(T_1). The recovered magnetization was determined either from the height of the quadrupolar echo obtained from a 'powdered-averaged' measurement, or from the amplitude of the perpendicular edge of the powder pattern. The T_1 values were determined by a linear least-squares analysis of eqn. (1) where

$$\ln[M_0 - M(T)] = -T/T_1 + \ln[M_0 - M(0)] \quad (1)$$

M_0 is the equilibrium magnetization, $M(T)$ is the magnetization at time T after the 180° pulse and $M(0)$ is the magnetization at $T = 0$.

The notation following Abragam's book[21] was used to describe the solid-state NMR frequency of an isolated deuteron by eqn. (2), where ω_0 is the Zeeman frequency and ω_Q is given

$$\omega = \omega_0 \pm \omega_Q \quad (2)$$

by eqn. (3).

$$\omega_Q = \frac{3}{4}\pi e^2qQ/h(3\cos^2\Theta - 1 - \eta\sin^2\Theta\cos 2\Phi) \quad (3)$$

e^2qQ/h is the quadrupolar coupling constant (QCC); the asymmetry parameter, η, describes the deviation of the electric field gradient (EFG) tensor from axial symmetry in the principal axis system (PAS) and Θ and Φ are the polar angles locating the magnetic field vector B_0 in the PAS of the EFG. The correlation time, τ_c, was determined using the following equation (eqn. (4)) ($\Theta = 70.5°$ and $\Phi = 90°$):

$$\frac{1}{T_1} = \frac{12\omega_Q^2}{81}\left(\frac{\tau_c}{1 + \omega^2\tau_c^2} + \frac{2\tau_c}{1 + 4\omega^2\tau_c^2}\right) \quad (4)$$

X-Ray crystallography

Crystal and molecular structures of **1** were determined using data collected at room temperature on a CAD4 diffractometer with graphite monochromatized Cu-Kα radiation.[22] Compound **1a** crystallizes in the monoclinic system, in space group $C2$, while **1b** crystallizes in the trigonal system, in space group $P3_2$. Crystal data and experimental details are shown in Table 1. CCDC reference number 188/176.

Acknowledgements

The authors are grateful to the Polish Committee of Scientific Research (KBN) for financial support, grant no. 3T09A11612.

References

1 J. M. Lehn, in *Supramolecular Chemistry*, *Concepts and Perspectives*, VCH, Weinheim, New York, Basel, Cambridge, Tokyo, 1995.
2 F. Vögtle, in *Supramolecular Chemistry*, John Wiley & Sons, Chichester, New York, Brisbane, Toronto, Singapore, 1991.
3 G. A. Jeffrey and W. Saenger, in *Hydrogen Bonding in Biological Structures*, Springer-Verlag, Berlin, Heidelberg, New York, 1991.
4 (*a*) G. R. Desiraju, *Acc. Chem. Res.*, 1991, **24**, 290; (*b*) G. R. Desiraju, *Acc. Chem. Res.*, 1996, **29**, 441; (*c*) G. R. Desiraju, *Angew. Chem., Int. Ed. Engl.*, 1995, **34**, 2311; (*d*) M. Zaworotko, *Chem. Soc. Rev.*, 1994, **23**, 283.
5 M. J. Potrzebowski, M. Michalska, A. E. Kozioł, S. Kaźmierski, T. Lis, J. Pluskowski and W. Ciesielski, *J. Org. Chem.*, 1998, **63**, 4209.
6 D. Braga, F. Grepioni, K. Biradha, V. R. Pedireddi and G. R. Desiraju, *J. Am. Chem. Soc.*, 1995, **117**, 3156.
7 M. T. Carroll and R. F. Bader, *Mol. Phys.*, 1988, **65**, 695.
8 M. J. Potrzebowski, J. Błaszczyk and M. W. Wieczorek, *J. Org. Chem.*, 1995, **60**, 2549.
9 WIN-MAS program, version 940108, Bruker-Franzen Analytik GMBH, Bremen, 1994.
10 (*a*) J. Herzfeld and A. Berger, *J. Chem. Phys.*, 1980, **73**, 6021; (*b*) G. Jeschke and G. Grossmann, *J. Magn. Reson.*, 1993, **A103**, 323.
11 (*a*) R. G. Griffin, *Methods Enzymol.*, 1981, **72**, 108; (*b*) L. W. Jelinski, in *High Resolution NMR Spectroscopy of Synthetic Polymers in Bulk*, Ed. R. A Komoroski, VCH Publishers, 1986, chap. 10, pp. 335–364.
12 G. L. Hoatson and R. L. Vold, in *NMR Basic Principles and Progress*, Ed. P. Diehl, E. Fluck, H. Günther, R. Kosfeld and J. Seelig, Springer-Verlag, 1994, Vol. 32, pp. 1–69.
13 (*a*) D. A. Torchia and A. Szabo, *J. Magn. Reson.*, 1982, **49**, 107; (*b*) D. A. Torchia and A. Szabo, *J. Magn. Reson.*, 1985, **64**, 135.
14 P. Dais and A. Perlin, *Can. J. Chem.*, 1983, **61**, 1542.
15 P. Dais, in *NMR of Biological Macromolecules*, NATO ASI Series, Ed. C. I. Stassinopoulou, Springer-Verlag Berlin, Heidelberg, 1994, Vol. H. 87, pp. 263–278.
16 K. Beshah, E. T. Olejniczak and R. G. Griffin, *J. Chem. Phys.*, 1987, **86**, 4730.
17 (*a*) L. Bachedlar, C. H. Niu and D. A. Torchia, *J. Am. Chem. Soc.*, 1983, **105**, 2228; (*b*) S. W. Sparks, N. Budhu, P. E. Young and D. A. Torchia, *J. Am. Chem. Soc.*, 1988, **110**, 3359; (*c*) A. Kintanar, T. M. Alam, W. C. Huang, D. C. Schindale, D. E. Wemmer and G. Drobny, *J. Am. Chem. Soc.*, 1988, **110**, 6367.
18 J. Mason, *Solid State Nucl. Magn. Reson.*, 1993, **2**, 285.
19 J. H. Davies, K. R. Bloom, M. I. Valic and I. P. Higgs, *Chem. Phys. Lett.*, 1976, **42**, 390.
20 M. S. Greenfield, A. D. Ronemus, R. L. Vold, R. R. Vold, P. D. Ellis and T. E. Raidy, *J. Magn. Reson.*, 1987, **70**, 89.
21 A. Abragam, *Principles of Nuclear Magnetism*, Oxford University Press, Stuttgart, 1961.
22 J. D. Schagen, L. Straver, F. Van Meurs and G. Williams, *CAD4 Manual. Version 5.0*, Enraf-Nonius, Delft, The Netherlands, 1989.

Paper 9/03119G